Electron. Mater. Lett., Vol. 11, No. 3 (2015), pp. 360-365
DOI: 10.1007/s13391-015-4442-1

Low Temperature Processed InGaZnO Oxide Thin Film Transistor Using Ultra-Violet Irradiation

S. H. Cho,[1] M. J. Choi,[2] K. B. Chung,[2,*] and J. S. Park[3]

[1]Department of Physics, Dankook University, Cheonan 330-714, Korea
[2]Division of Physics and Semiconductor Science, Dongguk University, Seoul 100-715, Korea
[3]Division of Materials Science and Engineering, Hanyang University, Seoul 133-791, Korea

(received date: 28 November 2014 / accepted date: 2 January 2015 / published date: 10 May 2015)

Device performance and bias stability of InGaZnO (IGZO) thin film transistors (TFTs) were investigated as a function of post-treatment with the combination of ultra-violet (UV) irradiation and thermal annealing. Under low temperature annealing at 150°C after UV irradiation, the device performance and bias stability of IGZO TFTs were enhanced with field effect mobility of 10.14 cm^2/Vs and ΔV_{th} below 0.5 V. The electrical characteristics of IGZO TFTs improved without a change in the physical structure and the origin of enhanced device performance can be explained by the changes of the oxygen coordination and the evolution of the electronic structures, such as the band edge states and band alignment of the Fermi level within the bandgap.

Keywords: oxide thin film transistor, ultra-violet irradiation, low temperature process, electronic structure

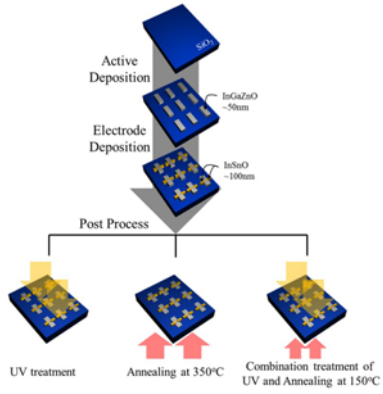

1. INTRODUCTION

Amorphous InGaZnO (IGZO) thin-film transistors (TFTs) have been attracted attention as an active channel layer of switching in devices for various electronic applications,[1] including active-matrix organic light emitting diodes (AMOLEDs),[2] liquid crystal displays (LCDs),[3] and gas sensors.[4] Compared to traditional amorphous/poly Si thin film transistors, amorphous oxide semiconductors (AOSs) that are based on TFTs have great advantages of low temperature and a low cost process as well as superior electron mobility and transparency.[5] For mass production to be practical, higher device performance and better device instability still remain as some of the most critical issues. Recently, many efforts have been made to seek alternative oxide semiconductors that have better device performance and stability under bias and illumination stress.[6-8] In addition, a low temperature process, which is below 200°C, is necessary for flexible and wearable electronics.[9] Several researchers have studied the improvement of device characteristics through the modifications of device structure, materials, and process parameters.[10-12] It has been shown that improvements to stability and performance of amorphous IGZO (a-IGZO) TFTs can be achieved by post-treatment on an insulator or channel layer. Examples of the post-treatment include thermal annealing, plasma treatment, and ultra-violet (UV) irradiation.[13-15] However, thermal annealing requires a high annealing temperature, usually over 300°C,[16] and the plasma treatment generates the plasma damage in order to obtain a reasonable device performance. Also, even if UV-ozone photo-annealing (below 300°C) and the combined plasma-microwave irradiation for solution-processed a-IGZO TFTs improve the device characteristics at the comparatively low temperature, the process time is long and the mobility is low compared with another process.[17,18] In addition, nitrogen high-pressure annealing and ion irradiation seem to have a better electrical mobility.[19,20] However, high pressure annealing has the relatively worse reliability and ion irradiation has the limitation of sample size due to the small ion beam area. These problems can restrict the compatibility and application to the flexible substrates and large size applications.

In this study, we focused to the improvement of device performance based on the simple process at low temperature with the minimized physical stress. The combination of UV

*Corresponding author: kbchung@dongguk.edu

irradiation and low temperature annealing were attempted on the channel-layer, so the device performance and instability of IGZO TFTs could be improved. The origins of electrical properties were interpreted with respect to the electronic structure of the band edge states below the conduction band and band alignment, which are correlated to the chemical bonding states.

A combination of UV irradiation and low temperature annealing at 150°C shows better device characteristics with smaller oxygen deficient states, smaller band edge states, and a smaller energy difference between the conduction band minimum and Fermi level.

2. EXPERIMENTAL PROCEDURE

Heavily doped P-type Si wafers with thermally grown SiO_2 (100 nm) were used as substrates onto which the InGaZnO (IGZO) films (50 nm) were deposited without the substrate being heating and by a radio frequency (RF) sputtering system. The RF power and process pressure were set to 75 W and 10 mTorr, respectively; these conditions were controlled by an Ar gas flow rate of 50 sccm. The active area was defined by using a shadow mask during the IGZO film deposition. After that, the indium-tinoxide (ITO) source/drain (S/D) electrode was deposited and re-patterned by using the shadow masks. The fabricated TFTs had a bottom-gate structure, and they also had a channel width (W) and length (L) of 1000 μm and 150 μm, respectively. Finally, the IGZO TFTs were post-processed with UV irradiation, 350°C annealing, and the sequential combination of UV irradiation and 150°C annealing. The schematic process diagram of prepared samples was systematically summarized in Fig. 1. Annealing of IGZO TFTs was performed by using a furnace system for 1 hour and, UV irradiation of the surface was carried out inside the chamber for 15 minutes. The wavelength and power density of the UV lamp are 254 nm and 17.69 mW/cm^2, respectively. In order to analyze the physical and electronic properties of IGZO films, separated IGZO films were prepared on identical substrates and underwent the same post-treatments as the TFT devices. The physical crystallization and its orientation of the post-treated IGZO films were observed by x-ray diffraction (XRD), and the surface morphology was investigated by using atomic force microscopy (AFM). Chemical bonding states were examined by x-ray photoelectron spectroscopy (XPS), which used a monochromatic AlKα source and had a pass energy of 20 eV. The electronic structures, which were related to changes in the band alignment and band edge states that below the conduction band, were investigated by XPS and spectroscopic ellipsometry (SE). The SE measurements were performed by a rotating analyzer system with an auto retarder, in the energy range of from 0.75 eV to 5.0 eV and with incident angles of 65°, 70°, and 75°.

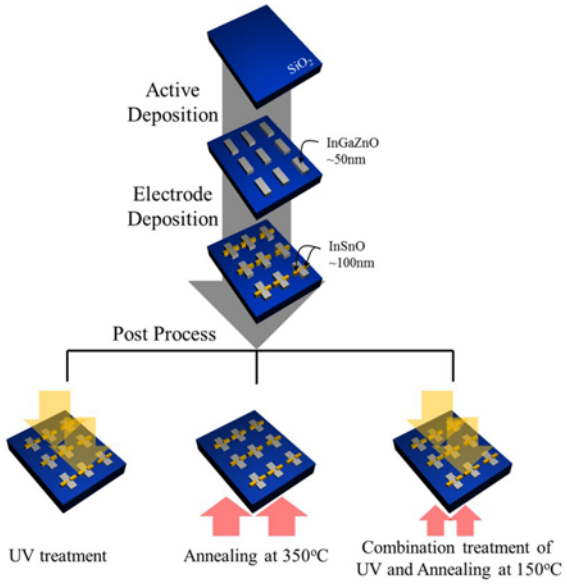

Fig. 1. Schematic process diagram of prepared samples. After the fabrication of TFTs, post process was divided by three different treatment ; only UV treatment (UV), only annealing at 350°C (350°C), and the sequential combination treatment of UV and annealing at 150°C (UV&150°C).

3. RESULTS AND DISCUSSION

Figure 2(a) and (b) show the representative transfer characteristics and the device parameters of the IGZO TFTs, depending on the post-treatment conditions. The field effect mobility (μ_{FE}) and threshold voltage (V_{th}) in the saturation region (V_{DS} = 10.1 V) were calculated by fitting a straight line to the plot of the square root of I_{DS} versus V_{GS}, according to the expression for a field effect transistor.[21] The subthreshold gate swing (S.S) value was extracted from the linear part of the log(I_{DS}) vs. V_{GS} plot.[22] The device performance had a significant improvement because of the post-treatment, which was a combination of UV irradiation and low temperature annealing at 150°C. Low temperature annealing of IGZO TFTs that were conducted after UV irradiation, enhanced the μ_{FE} and S.S values from 5.15 cm^2/Vs and 0.98 V/decade of the only UV irradiation to 10.14 cm^2/Vs and 0.49 V/decade, which are slightly higher than results obtained with a high temperature annealing at 350°C. These results imply that the combination of post-treatments are a critical factor in changing the charge-trapped defects in the IGZO semiconductor and/or interface (IGZO/SiO_2) because the field effect mobility and S.S values were improved.[14] The bias instability of the TFTs with IGZO active layers was also investigated as a function of post-treatment under negative bias stress (NBS) condition and with a gate bias of −20 V after 10, 100, 1000, and 3600 seconds, as shown in Figure 2(c). As the stress time increased, the transfer

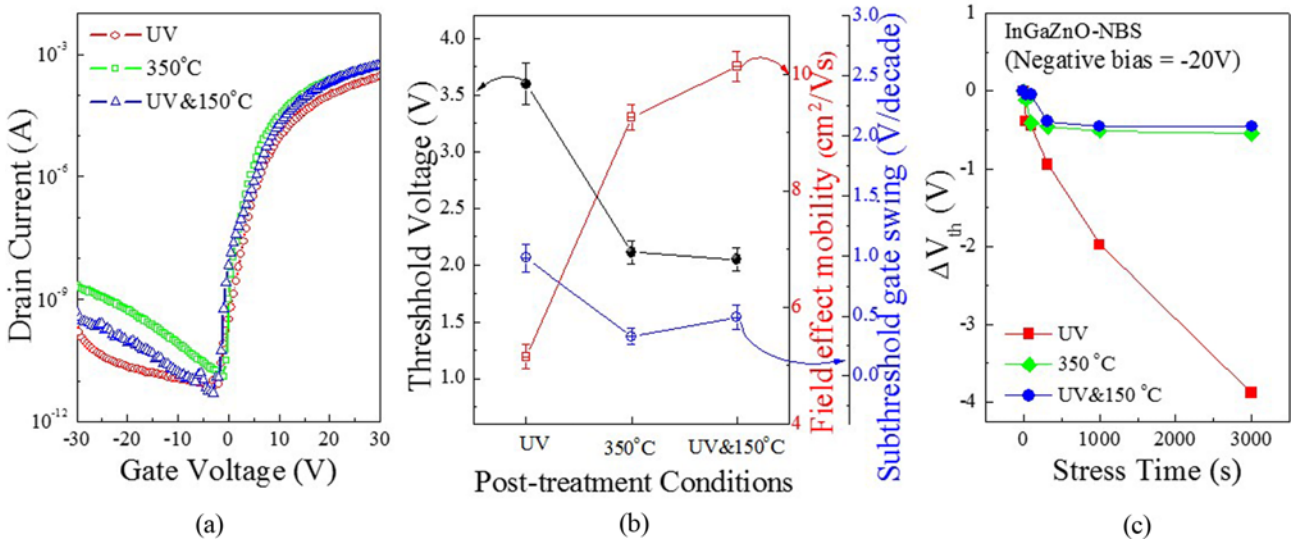

Fig. 2. (a) Transfer characteristics, (b) TFTs parameters including field effect mobility (μ_{FE}), and threshold voltage (V_{th}), subthreshold gate swing (S.S.), and (c) shift of threshold voltage under negative bias stress (−20 V) of IGZO TFTs with the W = 1000 μm and L = 150 μm as a function of post-treatments.

characteristics of IGZO TFTs systematically shifted in the negative direction, without any significant changes of mobility or S.S values. The annealing treatment at 350°C showed a smaller shift in the negative direction of the transfer curves as compared with the only UV irradiation. The combination treatments of low temperature annealing after UV irradiation improved the ΔV_{th} from −3.88 V to −0.45 V, as compared to the only UV irradiation, which had a corresponded value with the only annealing treatment at 350°C. This smaller shift of ΔV_{th} suggested that the charge trapping can be dominant in the bias instability of oxide TFTs, depending on the post-treatments, and the origin of charge trapping can be related to the oxygen-related traps in the channel and at the insulator/channel interface.

The physical structure and surface morphology were dependent on the post-treatments and were investigated by using XRD and AFM measurements, as shown in Fig. 3(a) and (b). Regardless of post-treatments, IGZO films had an amorphous structure. Also, surface morphology and roughness showed a small variation of RMS roughness with 0.349 nm, 0.324 nm, and 0.335 nm for the only UV irradiation, the only annealing at 350°C, and combination treatment of UV irradiation and low temperature annealing at 150°C, respectively. These changes mean that the physical structure and surface morphology have very little connection with the electrical device performance. In order to interpret the enhancement of device performance and instability in IGZO TFTs, more discussion is provided below and shows the electronic structure, including the chemical bonding states, band edge states that were below the conduction band, and band alignment.

The chemical bonding states were observed by XPS, and

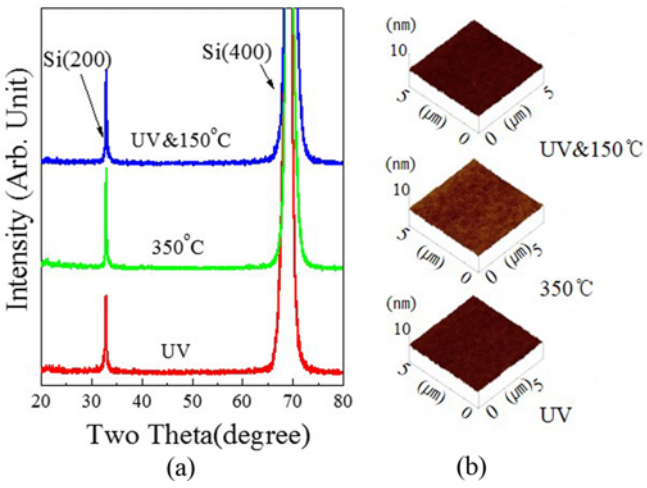

Fig. 3. (a) Physical structure, (b) surface roughness of IGZO films as a function of post-treatments.

the changes in oxygen 1*s* spectra are shown in Fig. 4. XPS spectra were measured after eliminating the surface contamination of adsorbed OH, C, H_2O, etc., and minimizing the preferred sputtering of light elements by using Ne ions at 500 eV. In order to differentiate the detailed oxygen states, the oxygen 1*s* spectra were carefully deconvoluted into three peaks (O1, O2, O3), by using a Gaussian fitting with the subtraction of a Shirley type background.[23] The low binding energy peak (O1) at 530.8 eV is related to the O^{2-} ions on the metal oxides, indicating In-Ga-Zn-O bonds. The higher binding energy peak (O3) around 532.8 eV is usually attributed to chemisorbed or dissociated oxygen or OH species on the surface of the IGZO films. The peak at the medium binding energy (O2) is associated with OH bonding

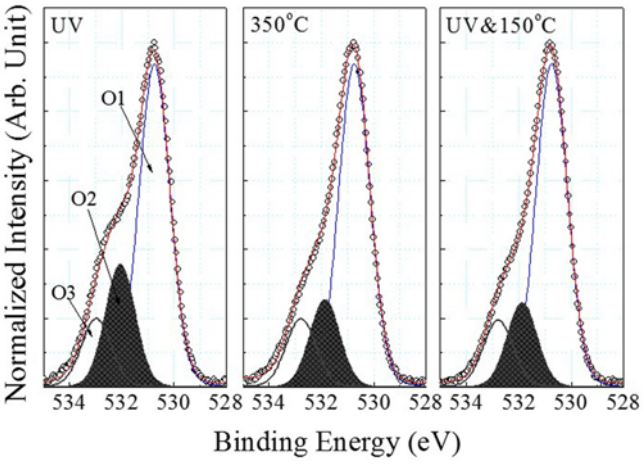

Fig. 4. Deconvoluted XPS O 1s core level as a function of post-treatments.

species and with O^{2-} ions that are in the oxygen-deficient In-Ga-Zn-O bonding matrix. The density of oxygen deficient bonding state (O2) decreased in the combination treatment of UV irradiation and low temperature annealing at 150°C as compared to the only UV irradiation and the only annealing at 350°C. This result implied that the IGZO films that were post-treated by combination of UV irradiation and low temperature annealing have smaller oxygen-related defects that were generated by the oxygen deficient bonding state (O2), possibly causing the improvement of the device performance and instability.[24]

In order to understand the electronic structure of the IGZO films, including the bandgap and band edge states that were below the conduction band, complex dielectric function ($\varepsilon = \varepsilon_1 + i\varepsilon_2$) were obtained by using SE as a function of post-treatment conditions in Fig. 5. These spectra were extracted

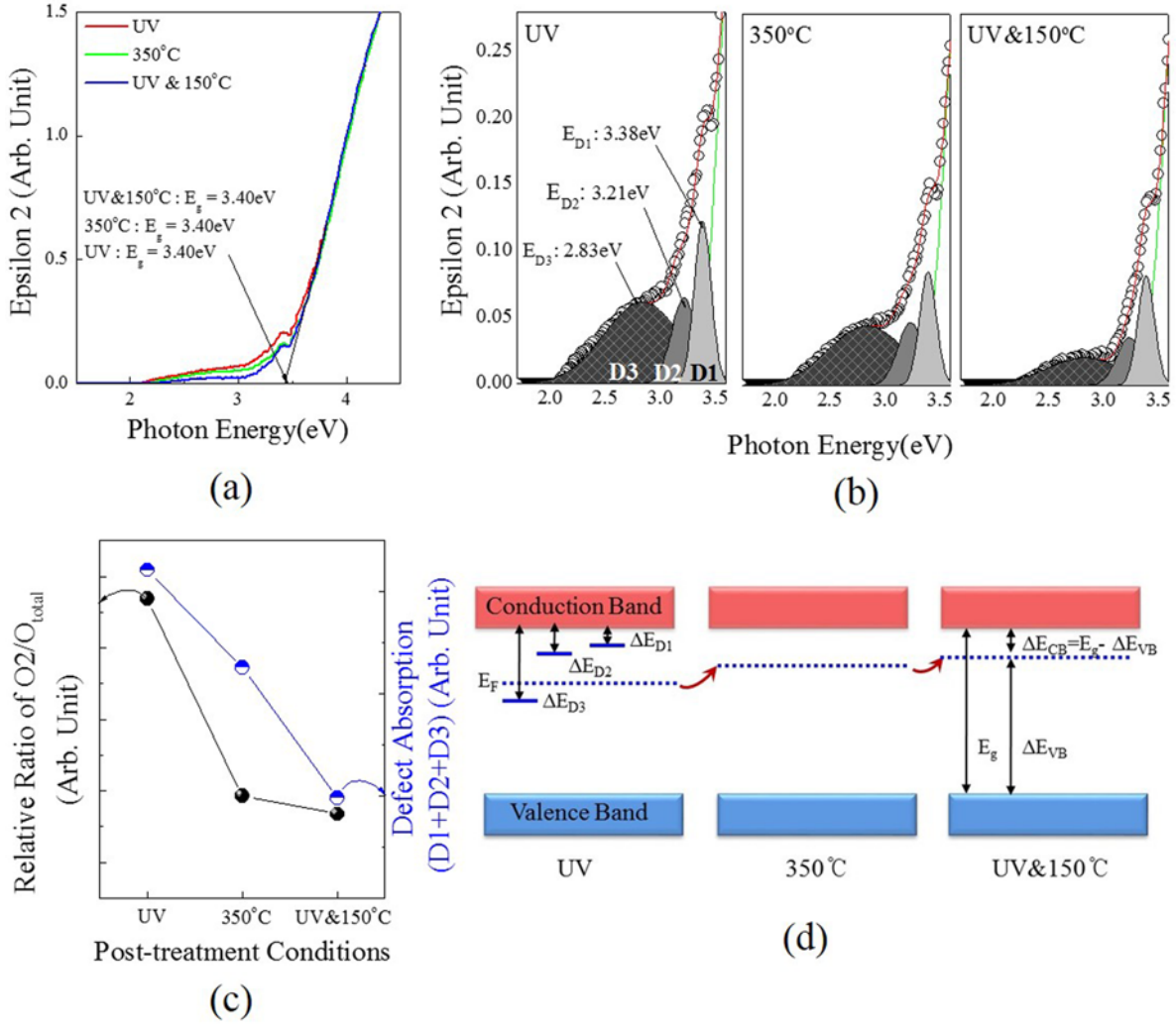

Fig. 5. (a) Imaginary dielectric function (ε_2) spectra, (b) band edge states over a narrow energy region and below the conduction band edge, (c) qualitative comparison between the relative ratio of $O2/O_{total}$ from XPS O 1s spectra and defect absorption of band edge states from SE measurement, and (d) schematic energy level diagram that reflect the relative energy position of the Fermi level (E_F) and band edge states (D1, D2, D3), with respect to the conduction band minimum as a function of post-treatments.

from a simple four-phase model, which consisted of a substrate, SiO_2 layer, IGZO overlayer, and an ambient layer. Figure 5(a) shows the imaginary dielectric function (ε_2) spectra. The optical bandgap of IGZO films has a similar value ~3.40 eV, regardless of post-treatments. These interesting findings are changes of the unoccupied absorption states within the bandgap, which are getting to smaller in the combination treatments. Gaussian fits that used three different peaks (D1, D2, D3) were performed in the region of the band edge states; the detailed examination are shown in Fig. 5(b). According to the post-treatments, the evolution of the band edge states proved that the shallow band edge states (D1), (D2) decreased, and, especially, the deep band edge state (D3) drastically decreased, which is totally related to the decrease of oxygen deficient chemical bonding states as shown in the XPS results of Fig. 4.[25,26] Figure 5(c) shows the relative density of oxygen deficient bonding states (O2) and the defect absorption of band edge states (D1, D2, D3) as a function of post-treatments. The combination of UV irradiation and low temperature annealing at 150°C induced the decrease of oxygen deficient state and band edge states that are within the bandgap, which are strongly related to the enhancement of mobility and improvement of instability because of the lower possibility of charge trapping being in the unoccupied states that are within the bandgap.[24] Figures 5(d) show the schematic energy diagram for IGZO films by using SE and XPS as a function of post-treatment conditions. The corresponding values of the band-gap (E_g), the valence band offset (ΔE_{VB}) between the valence band maximum and Fermi level (E_F), the conduction band offset (ΔE_{CB}) between the E_F and conduction band minimum, and relative energy levels of defect states from conduction band minimum (ΔE_{D1}, ΔE_{D2}, ΔE_{D3}) as a function of post-treatments are summarized in Table 1. Even if the defect densities are changed as shown in Fig. 5(a) and (b), there was no energy shift of ΔE_{D1}, ΔE_{D2}, or ΔE_{D3} regardless of the post-treatments. On the other hand, the conduction band offset (ΔE_{CB}) was changed from 0.49 eV to 0.31 eV, depending on the post-treatments. The combination of UV irradiation using 254 nm (4.88 eV) and low temperature annealing at 150°C is enough energy because of higher energy than the bandgap, to excite the electron and to reduce the activation energy of electron from the occupied states, which causes the smaller unoccupied band edge states and smaller oxygen deficient states. Thus, these evolutions enhance the electrical conductivity due to the less electron trapping, in addition to the smaller transition energy from Fermi level to unoccupied conduction band.

Table 1. Summary of band alignments of InGaZnO films for the bandgap (E_g), the valence band offset (ΔE_{VB}) between the valence band maximum and Fermi level (E_F), the conduction band offset (ΔE_{CB}) between the E_F and conduction band minimum, and the relative energy levels of defect states from the conduction band minimum (ΔE_{D1}, ΔE_{D2}, ΔE_{D3}), all of which as a function of post-treatments.

Treatments	E_g (eV)	ΔE_{VB} (eV)	ΔE_{CB} (eV)	ΔE_{D1} (eV)	ΔE_{D2} (eV)	ΔE_{D3} (eV)
UV	3.40	2.91	0.49	0.02	0.19	0.57
350°C	3.40	3.07	0.33	0.02	0.19	0.57
UV&150°C	3.40	3.09	0.31	0.02	0.19	0.57

4. CONCLUSIONS

In summary, the device performance and bias stability of InGaZnO (IGZO) thin film transistors (TFTs) were investigated as a function of post-treatment with the combination of ultra-violet (UV) irradiation and low temperature annealing at 150°C. Compared to other post-treatment conditions, such as UV irradiation or high temperature annealing at 350°C, low temperature annealing of IGZO TFTs after UV irradiation enhanced the device performance and bias stability with field effect mobility of 10.14 cm^2/Vs, a subthreshold slope (S.S) of 0.49 V/decade, a threshold voltage (V_{th}) of 2.05 V, and ΔV_{th} below 0.5 V. The improvement of TFTs properties without structural transformation is explained by the changes of the oxygen coordination and electronic structures, including oxygen bonding states, the band edge states, and band alignment of Fermi level within the bandgap. Under the post-treatment which was the combination of UV irradiation and low temperature annealing, IGZO film had smaller oxygen deficient bonding states and band edge states. In addition, the Fermi level (E_F) is relocated to the shallow energy level from the conduction band minimum, which induced the smaller conduction band offset (ΔE_{CB}). These evolutions of the electronic structure are strongly correlated to the device characteristics of IGZO TFTs, depending on the UV irradiation and thermal annealing. From our results, the combinatorial post-treatments at low temperature can be applied, with a simple modification of previous process, to the flexible and wearable electronics

ACKNOWLEDGEMENTS

This research was supported by the Basic Science Research Program through the National Research Foundation of Korea (NRF) funded by the Ministry of Education, Science and Technology (NRF-2013R1A1A2A10005186).

REFERENCES

1. T. Kamiya, K. Nomura, and H. Hosono, *Sci. Technol. Adv. Mater.* **11**, 044305 (2010).
2. J. K. Jeong, J. H. Jeong, J. H. Choi, J. S. Im, S. H. Kim, H. W. Yang, K. N. Kang, K. S. Kim, T. K. Ahn, H. J. Chung, M. K. Kim, B. S. Gu, J. S. Park, Y. G. Mo, H. D. Kim, and H. K. Chung, *SID* **39**, 1 (2008).

3. J. S. Park, W. J. Maeng, H. S. Kim, and J. S. Park, *Thin Solid Films* **520**, 1679 (2012).
4. D. J. Yang, George C. Whitfield, N. G. Cho, P. S. Cho, I. D. Kim, Howard M. Saltsburg, and Harry L. Tuller, *Sens. Actuators B, Chem.,* **171**, 1166 (2012).
5. K. Nomura, H. Ohta, A. Takagi, T. Kamiya, M. Hirano, and H. Hosono, *Nature* **432**, 488 (2004).
6. J. S. Park, K. Kim, Y. Park, Y. Mo, H. D. Kim, and J. K. Jeong, *Adv. Mater.* **21**, 329 (2009).
7. K. M. Lee, G. W. Ko, G. H. Lee, G. B. Han, M. M. Sung, T. W. Ha, J. H. Kim, and S. I. Im, *Appl. Phys. Lett.* **97**, 082110 (2010).
8. B. D. Ahn, K. C. Ok, J. S. Park, and K. B. Chung, *J. Vac. Sci. Technol. B.* **31**, 021204 (2013).
9. M. G. Kim, Mercouri G. Kanatzidis, A. Facchetti, and T. J. Marks, *Nature Mater.* **10**, 382 (2011).
10. X. Li, E. Xin, and J. Zhang, *Electron. Mater. Lett*. **11**, 143 (2015).
11. B. S. Yang, M. S. Hur, S. Oh, U. S. Lee, Y. J. Kim, M. S. Oh, J. K. Jeong, C. S. Hwang, and H. J. Kim, *Appl. Phys. Lett.* **98**, 122110 (2011).
12. H. Y. Huang, S. J. Wang, C. H. Wu, and C. Y. Lu, *Electron. Mater. Lett.* **10**, 899 (2014).
13. L. Li, L. Fan, Y. Li, Z. Song, F. Ma, and C. Liu, *J. Vac. Sci. Technol. A.* **32**, 021506 (2014).
14. J. S. Kim, M. K. Joo, M. X. Piao, S. E. Ahn, Y. H. Choi, H. K. Jang, and G. T. Kim, *J. Appl. Phys.* **115**, 114503 (2014).
15. H. W. Zan, W. T. Chen, C. W. Chou, C. C. Tsai, C. N. Huang, and H. W. Hsueh, *Electrochem. Solid-State Lett.* **13**, H144 (2010).
16. H. S. Shin, B. D. Ahn, K. H. Kim, J. S. Park, and H. J. Kim, *Thin Solid Films* **517**, 6349 (2009).
17. Y. H. Hwang, K. S. Kim, and W. J. Cho, *Jpn. J. Appl. Phys.* **53**, 04EF12 (2014).
18. B. Y. Su, S. Y. Chu, Y. D. Juang, and H. C. Chen, *Appl. Phys. Lett.* **102**, 192101 (2013).
19. S. H. Yoon, Y. J. Tak, D. H. Yoon, U. H. Choi, J. S. Park, B. D. Ahn, and H. J. Kim, *ACS. Appl. Mater. Interfaces*, **6**, 13496 (2014).
20. B. D. Ahn, J. S. Park, and K. B. Chung, *Appl. Phys. Lett.* **105**, 163505 (2014).
21. J. S. Park, J. K. Jeong, Y. G. Mo, H. D. Kim, and C. J. Kim, *Appl. Phys. Lett.* **93**, 033513 (2008).
22. J. H. Jeong, H. W. Yang, J. S. Park, J. K. Jeong, Y. G. Mo, H. D. Kim, J. W. Song, and C. S. Hwang, *Electrochem. Solid-State Lett.* **11**, H157 (2008).
23. B. D. Ahn, J. H. Lim, M. H. Cho, J. S. Park, and K. B. Chung, *J. Phys. D* **45**, 415307 (2012).
24. H. W. Park, B. K. Kim, J. S. Park, and K. B. Chung, *Appl. Phys. Lett.* **102**, 102102 (2013).
25. H. Seo, C. J. Park, Y. J. Cho, Y. B. Kim, and D. K. Choi, *Appl. Phys.Lett.* **96**, 232101 (2010).
26. B. K. Kim, J. S. Park, D. H. Kim, and K. B. Chung, *Appl. Phys. Lett.* **104**, 182106 (2014).